Microstructural Analysis of Intermetallic Ni_5Al_3 Thin Films

T. Joseph Sahaya Anand[1], A.H.W. Ngan[2]

[1]Faculty of Manufacturing Engineering, Universiti Teknikal Malaysia Melaka, Locked Bag 1752, Pejabat Pos Durian Tunggal, 76109 Durian Tunggal, Melaka, Malaysia.

[2]Department of Mechanical Engineering, University of Hong Kong, Pok Fu Lam Road, Hong Kong.

ABSTRACT

The possible magnetic transition phenomenon obtained is postulated particularly on the Nickel Aluminum (Ni_5Al_3) thin films of different thickness. It was found that the film resistance exhibits a linear but mild increase over the initial temperature range, followed by a transition to a relatively rapid decline in the resistance after attaining maximum at ~170ºC. This positive temperature coefficient of resistance (TCR) makes this material suitable for magneto resistor applications. The same observations were made on two different sputtering systems with different deposition conditions, indicating that the magnetic transition is a highly reproducible phenomenon.

KEYWORDS: *Magnetic transition, Alloys, Sputtering, Resistivity, PTC Thermistor,Nanocrystalline.*

1.0 INTRODUCTION

Magnetoresistor based shape memory alloys are of recent interest for their good temperature properties (Chan et al., 2007), (Vopálenský et al., 2007), (Wolkenberg and Przesławski, 2006), (Dimitrova et al., 2008). Ferromagnetic-to-Paramagnetic (FM-PM) transition is not a fascinating phenomenon since any ferromagnetic materials, pure Ni and ferrite permanent magnets for examples will lose their magnetic order when heated up to their respective transition temperatures. Ferromagnetism, to its simplest sense, is the state of a material to be strongly attracted to a magnetic field. This is related to a spontaneous re-orientation of the magnetic moments, or electronic spin states, of the atoms/ions to align with the applied field. Upon heating to beyond certain temperature, however, the atoms lose their preferred magnetic moments and turn into paramagnetic, where the material is only slightly attracted to a magnetic field. The temperature at which the magnetic

transition occurs is called the Curie temperature, or sometimes referred as the magnetic transition temperature.

There are some physical properties that will change at the instance the transition occurs: linear expansion coefficient and specific heat capacity are two of them. They normally show a discontinuity (narrow sharp peak) across T_c, and return to their original values afterwards. Besides a magnetic disorder, it seems to be that there are no other physical properties that will change drastically for general materials beyond their Curie temperatures. Recently FM-PM transition has been under substantial research on a range of magnetic thin film materials, including $La_{0.67}Ca_{0.33}MnO_3$ (LCMO), $La_{1-x}Sr_xMnO_3$ (LSMOP) and $La_{1-x}Sr_xCoO_3$ (LSCO) (Miao et al., 2008), (Gaur and Varma, 2008), (Grishin et al., 1999), (Khartsev et al., 2000), which find potential applications in electronics. This range of materials exhibits a "colossal" magnetoresistance effect that behaves interactively with their FM-PM transitions. Also polycrystalline $BaTiO_3$ and $(Sr_{1-x}Pb_x)$ TiO3 ferroelectric materials (NTC-PTC-NTC) as temperature increases (Huo and Qu, 2006, Lu and Tseng, 1998, Han et al., 2007, Zhao et al., 2001, Li et al., 2009, Shahrani and Abboudy, 2000). One of the potential explanations could be the effect of ferroelectricity or ferromagnetism-both phenomena that have been identified to be the origin of the reported temperature-coefficient-of-resistance (TCR) transitions in the above mentioned oxide materials.

This paper reports a magnetic anomaly observed on Ni_5Al_3 alloy thin films. Ni-Al coatings with a 3:1 stoichiometry that have been investigated in our previous work (Ng and Ngan, 2000) on conducting metal (Ni) substrates. Although the Ni-Al alloy films confirm to a normal metallic conductivity when either in its single phase or the thickness is well above 1 micron an abnormally high electrical resistance is exhibited at room temperature. It is observed when the film is thinner than a few hundred nanometers. The electrical resistance reduced drastically, when the film is heated up. The aim of the present work is to characterize the positive temperature coefficient of resistance (PTCR) in the Ni_5Al_3 alloy films.

2.0 EXPERIMENTAL DETAILS

The Ni_5Al_3 alloys for use as sputtering targets were prepared by casting commercially pure Ni (> 99.5 %) and Al (> 99.5 %) in the corresponding stoichiometric ratios at 1550ºC. These Nickel aluminium thin films were synthesized by a water-cooled, low-power dc magnetron sputtering device (BAL-TEC MED 020) using the corresponding nickel aluminium alloy targets. The sputtering chamber was evacuated with the base pressure maintained at well below 1×10^{-5} mbar, and a continuous flux of ultra high purity (> 99.9999 %) argon was introduced at a pressure of 5×10^{-2} mbar during film deposition.

Pre-sputtering of the target was performed at least three times with duration of 10 minutes each time, followed by flushing with high-purity argon to remove excess oxygen and other residual gases. Polished pure nickel plates with size 15 mm × 10 mm × 1 mm were used as substrates in most cases. In few cases, glass micro-slides or silicon wafers with similar dimensions were also used as substrates for compositional analyses by energy dispersive X-ray (EDX). The change of the substrate to glass or Si was to avoid signals from an otherwise Ni substrate to confuse with signals from the film itself. Prior to depositions, all the substrates were cleaned thoroughly by chemical and mechanical means to remove any organic contaminations on the surfaces. The Ni_5Al_3 alloy films were deposited at a sputtering power of 30 W and the alloy target was placed 60 mm above the substrate stage. Although there was no additional thermal source applied to the substrates during the deposition process, the substrates became warmed and were heated up nearly 60ºC due to the plasma-discharge heating. The deposition rate was measured to be approximately 2 – 3 Å/sec and the film thickness was controlled by means of deposition time.

Apart from the BAL-TEC MED 020 system in Hong Kong, films with the same compositional range were also prepared by a similar dc magnetron sputterer (JCK-500A) located at Nanjing University. In the Nanjing system, the working argon was introduced at 1 x 10^{-2} mbar after the residual gas pressure was pumped down to 2 x 10^{-5} mbar. The sputtering conditions were set at 60 watt, bias of 350 V and room temperature.
X-ray analyses of the films were conducted using a Siemens diffractometer with a CuKα target operating at 40 kV / 20 mA. To determine the film thickness, a special batch of nickel substrates was prepared with notches on the back and was fractured after deposition. The compositions of the Ni-Al thin films were determined by energy dispersive X-ray analyses (EDX). These results were also confirmed by wavelength dispersive analyses (WDS) in an electrical probe (JEOL JXA-8800). The surface chemistry of the films was analyzed by X-ray photoelectron spectroscopy (XPS) performed in a 300 W ESCALAB mk-II XPS spectrometer using an Al/Mg anode.

The electrical resistance at varying temperatures was measured for the Ni-Al thin films by a two-point-probe technique. The deposited specimens were rested on a hot plate and the electrical resistance was measured using a high accuracy digital ohmmeter (Tektronix DM 257). The temperature of the films was monitored by a surface contact type thermocouple mounted on the top of the specimens. The power of the heater was gradually controlled such that the samples were heated up at a sufficiently low speed (less than 0.5°C / sec) to ensure a minimal temperature gradient across the sample during resistance measurement.

Microstructural examination was carried out in a JEOL 2000-FX TEM operating at 200 kV as well as a Philips Tecnai TEM. It is very essential that the sample to be thin enough for the electrons to penetrate. For instance, it should not be thicker than 200nm, for a TEM having an electron gun of 200kV. The crystal structures of the films were analyzed by selected area diffraction (SAD). *In situ* annealing inside the TEM was carried out on as-deposited films to study the microstructural changes during heating. Post-deposition heat treatment of the films was carried out with a Carbolite vacuum furnace at a vacuum of about 1×10^{-6} mbar for 2 hours followed by furnace cool to enhance their crystallinity in the TEM for comparison purposes.

3.0 RESULTS

3.1 Structural and Compositional Characterization

The X-ray spectra of the as-deposited and annealed Ni_5Al_3 films on both glass microslides and nickel substrates are shown in Figure 1 (a-d). In the thicker films (~5 µm thick), peaks corresponding to the Ni_5Al_3 phase with an orthorhombic structure (Khadkikar and Vedula, 1987), which consists of four differently ordered f.c.c. unit cells, can be identified from the X-ray spectra. The presence of the Ni_5Al_3 phase in the films on both the conducting nickel substrates as well as on glass microslides was confirmed by XRD. In general the intensity of the peaks in the XRD patterns in Figure 1 increased with high temperature annealing, except that they did not correspond to any major changes in the lattice constants. Table 1 comprises the summary of results showing the theoretical 2θ values for different equilibrium Ni_5Al_3 results with the pure Ni data for comparison.

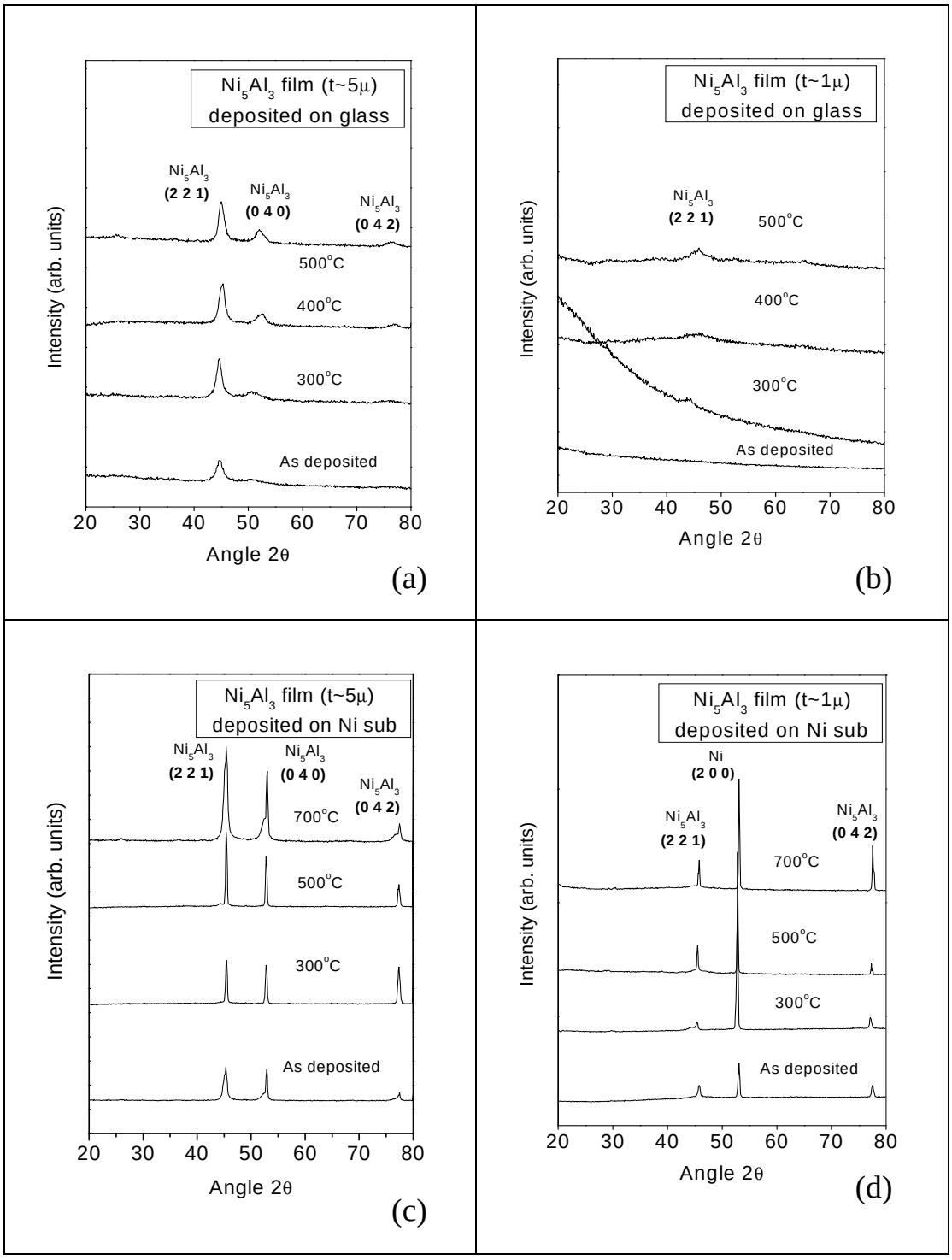

FIGURE 1
XRD spectra of Ni_5Al_3 thin films deposited on glass with thickness (a) t ~ 5μ (b) t ~ 1μ and on nickel substrate with thickness (c) t ~ 5μ and (d) t ~ 1μ

TABLE 1
Theoretical XRD lattice parameters of Ni_5Al_3 phases with $\lambda = 0.1542$ nm with the comparison data of Ni phase.

System	d (nm)	Angle (2θ)	Intensity	(h k l)
Ni_5Al_3 (Orthorhombic) a = 0.7475 nm; b = 0.6727 nm; c = 0.3732 nm	0.3367	26.471	2	0 2 0
	0.2643	33.917	4	2 0 1
	0.2081	43.486	100	2 2 1
	0.1869	48.720	35	4 0 0
	0.1869	48.720	35	0 0 2
	0.1684	54.488	11	0 4 0
	0.1635	56.263	1	4 2 0
	0.1635	56.263	1	0 2 2
	0.1321	71.404	9	4 0 2
	0.1249	76.226	21	4 4 0
	0.1249	76.226	21	0 4 2
	0.1114	87.579	20	2 2 3
	0.1037	96.043	10	4 4 2
Ni (Cubic; a = 0.3524 nm)	0.2034	44.505	100	1 1 1
	0.1762	51.844	42	2 0 0
	0.1246	76.366	21	2 2 0
	0.1062	92.939	20	3 1 1
	0.1017	98.440	7	2 2 2

Quantitative EDX and WDS analyses were performed to measure the relative abundance of nickel and aluminum in the sputtered Ni_5Al_3 thin films. The results in Table 2 show that the Ni and Al compositions of the films essentially comply with the range over which the corresponding intermetallic Ni_5Al_3 compounds would exist. It can be seen that the EDX and WDS results agree very well with one another.

TABLE 2
Compositional analysis of Ni-Al alloy films by EDX and WDS.

Nominal composition	Relative compositions of Ni_5Al_3 thin films (at. % ± 0.5 %)			
	EDX		WDS	
	Ni	Al	Ni	Al
$Ni_{0.65}Al_{0.35}$	65.1	34.9	65.1	34.9

In addition to the elements mentioned above, a noticeable amount of oxygen was detected by EDX analyses performed in the thin-window mode, which allows elements with atomic numbers smaller than 12 to be detected. Figure 2 shows typical

EDX spectra of the Ni_5Al_3 thin films with pure Ni_5Al_3 alloy target for comparison. It can be seen that remarkable oxygen peaks were detected mainly in the high-thickness, as-deposited films in the all compositions. But there was no significant amount of oxygen incorporated in the target materials as shown in Figure 2(c). This suggested that oxygen was incorporated into the film during sputtering. Unfortunately, owing to the limitation of the EDX quantitative analysis system, quantification of the composition for elements with atomic number smaller than 12 cannot be done. Alternatively, we can simply estimate the oxygen content by comparing the area under the oxygen peak with others, say, the Ni peak. The comparison shows that the oxygen content in the films is fairly constant.

A significant amount of oxygen (12 at. %) was observed in the as-deposited state but the oxygen content significantly reduced to 3.1 at. % after annealing at 500°C. The thicker film in Figure 2 (c) had even higher oxygen content of 29–34 at. % in the as-deposited state, but again the oxygen content reduced significantly after annealing at 300°C and 500°C for 2 hours. The oxygen content reduced from 30 to 17 at. % after annealing at 500°C.

In general, the oxygen content of the films can be reduced considerably either by post-deposition annealing as illustrated above, or by reducing the chamber pressure during deposition. The films prepared under a base pressure of 4.0×10^{-6} mbar were found to have their oxygen content reduced significantly to 5 – 8 %, as compared to the films prepared under a base pressure of 1.0×10^{-5} mbar. From the consideration that the initial target materials did not have any significant amounts of oxygen (Figure 2 (c)) but significant amounts of oxygen were observed in the deposited films, there is a possible leakage at the joining parts of the sputtering system. But the films prepared using another dc magnetron sputterer (JCK-500A) located in Nanjing University also contained significant amounts of oxygen. In fact, the films prepared in Nanjing were found to contain even more oxygen than those prepared using the BAL-TEC system in Hong Kong. This could be possibly due to the higher chamber base pressure (2.0×10^{-5} mbar) in the Nanjing machine.

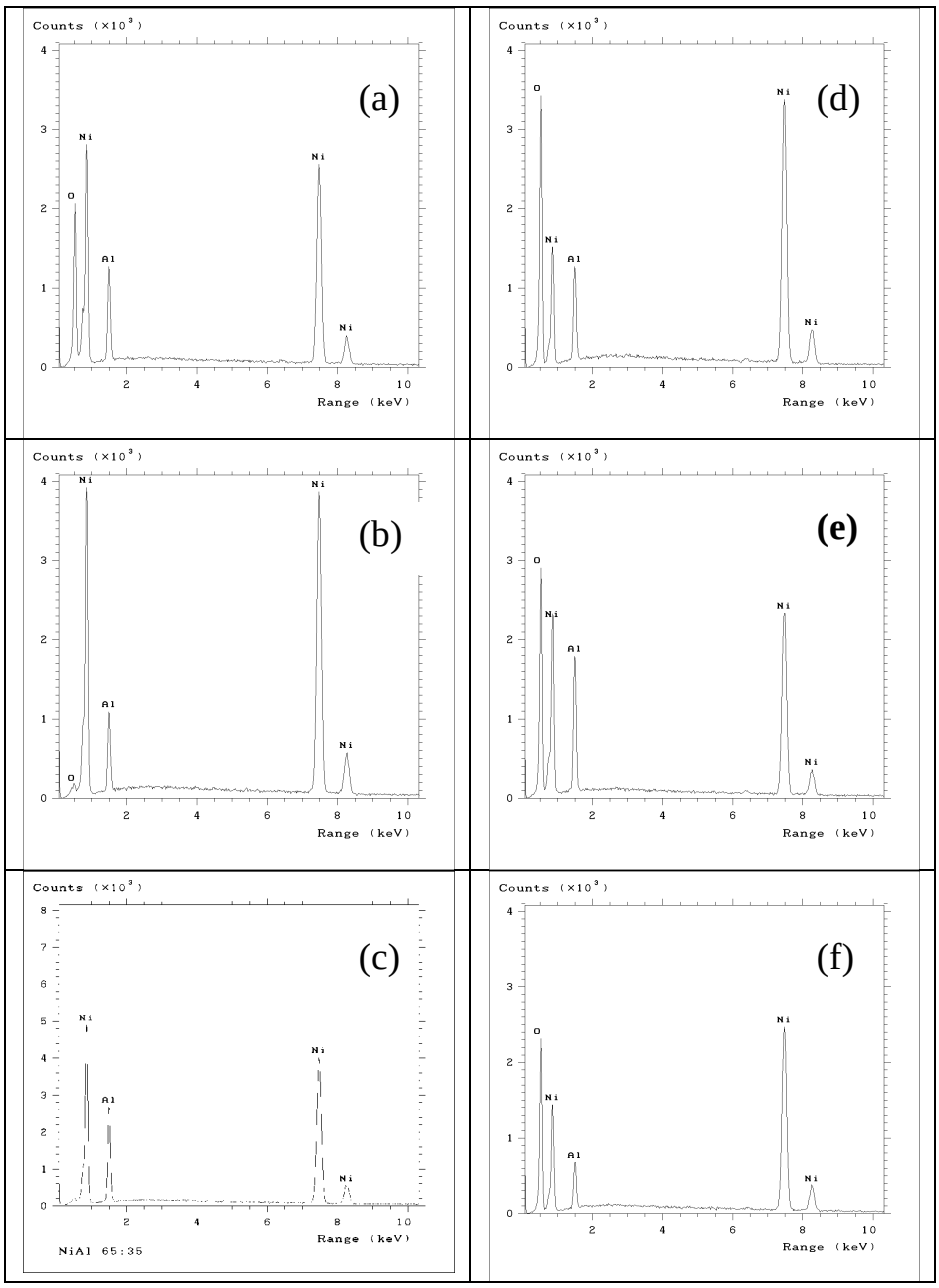

FIGURE 2

EDX spectra collected for Ni_5Al_3 thin films coated on glass substrates with low thickness approx. 230 nm (a) as deposited and vacuum annealed (b) 500°C with (c) Ni_5Al_3 target and high thickness > than 1 µm (d) as deposited and vacuum annealed (e) 300°C and (f) 500°C.

The oxygen content was also observed during X-ray photoelectron spectroscopy (XPS) analyses. Figure 3 represents the XPS spectra obtained from the as-deposited Ni_5Al_3 film. The binding energies have been corrected for specimen charging effect

by taking the C1s reference peak at 284.4 eV (Crist, 2000). From amongst the wide scan spectra, significant oxygen contents can be identified in all the specimens according to the pronounced oxygen 1s (O1s) peak observed at about 531 eV. Finely resolved spectra (left insets) of the Ni3p and Al2p regions indicate that Ni and Al existed in both of their respective metallic and higher valence states. In all the three film compositions, metallic Al (72.7 eV) was found to exist more preferentially than Al^{3+} (74.3 eV for Al_2O_3), whereas Ni was, on the contrary, enriched in its oxidized form especially for the Ni-rich specimens. The prevalence of Ni^{2+} is further illustrated by the $Ni2p_{3/2}$ peak (right insets), which extends through the relevant binding energies of metallic (852.8 eV) and oxidized (854.3 eV for NiO) nickel species. The emergence of satellite accompanying the Ni2p signal also infers the occurrence of Ni oxidants (Castle, 2002).

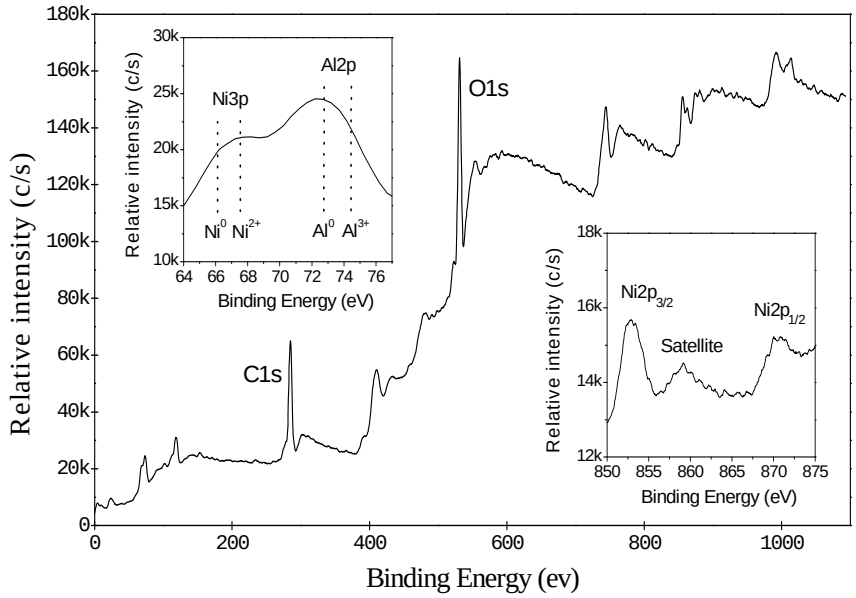

FIGURE 3
XPS spectra of Ni_5Al_3 thin films with the thickness less than 100 nm.

3.2 Electrical Resistance-Temperature Characteristics

Figure 4 (a) shows the typical resistance-temperature characteristics of the Ni_5Al_3 film prepared using the Hong Kong sputterer during a series of heating and cooling cycles. The film resistance exhibits a transition from positive to negative TCR behavior and this value of resistance exhibits a linear but mild increase over the initial temperature range, followed by a transition to a relatively rapid decline in resistance after peaking at ~170 °C. The positive TCR segments of the resistance

profiles of the Ni_5Al_3 film exhibit an averaged slope of +0.001 kΩ/°C, corresponding to a TCR of approximately $+2.7\times10^{-4}$/°C, whereas the subsequent negative TCR after the transition is estimated to be $-2.1\sim2.4\times10^{-3}$/°C over the range of temperature range concerned. The overall resistance of Ni_5Al_3 films lies in the kilo-Ω range, which confirms the similar results obtained by the other sputterer by the positive to negative TCR transition behavior as shown in Figure 4(b).

3.3 Nano-crystalline structure by transmission electron microscope

To study the structural properties of Ni_5Al_3 intermetallic thin films, SEM has inadequate capability to resolve the film microstructures with sufficient details. TEM was chosen to examine the nano-crystalline structure and internal build-up of the films to a finer extent. For this purpose, Ni_5Al_3 films were deposited on carbon films supported by copper grids to produce plan-view samples thin enough for electron transmission in the TEM. To study the grain growth kinetics as a function of time and temperature, dynamic microstructural observations were carried out on the TEM specimens during a series of isothermal *in situ* heat treatments.

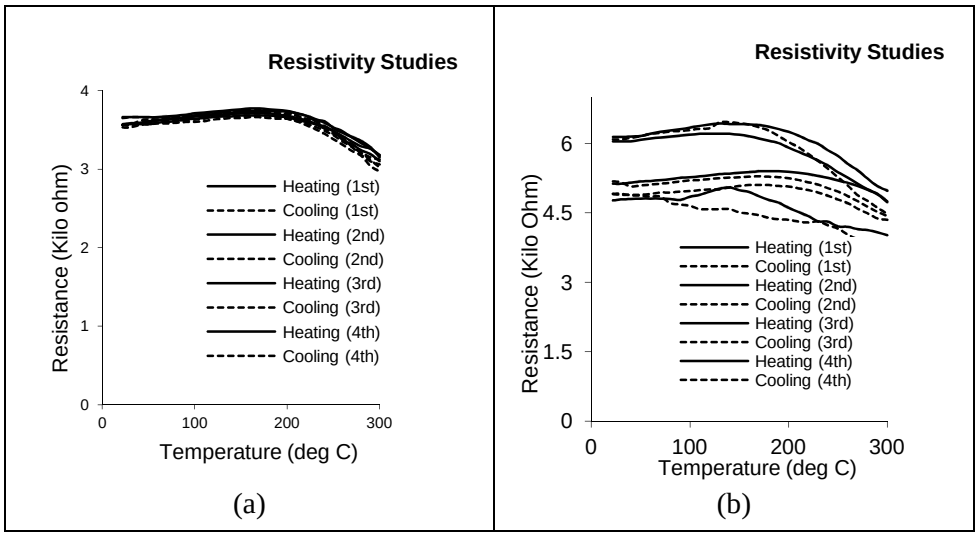

FIGURE 4

The resistance-temperature plots of Ni_5Al_3 films on Ni under a series of heating and cooling cycles (a) BAL-TEC MED 020 sputterer (thickness ~ 350 nm) (b) JCK-500A sputterer (thickness ~ 350 nm)

Figurer 5 and 6 show the *in situ* and post-deposition annealed transmission electron microscope analysis of Ni_5Al_3 thin films with thickness of approximately 150 nm. During the *in situ* annealing process at around 350°C, grain growth can be detected; the grain growth is uniformly distributed and there is no abnormal grain growth. However, the post deposition annealing results shows the grain size increment from a few nanometers initially to about 40 nm for the 700°C annealed specimen. The

intermediate phase Ni_5Al_3, which is orthorhombic and is stable below 700°C in the bulk condition, was observed throughout the process as shown in the corresponding SAD patterns and crystallographic calculations.

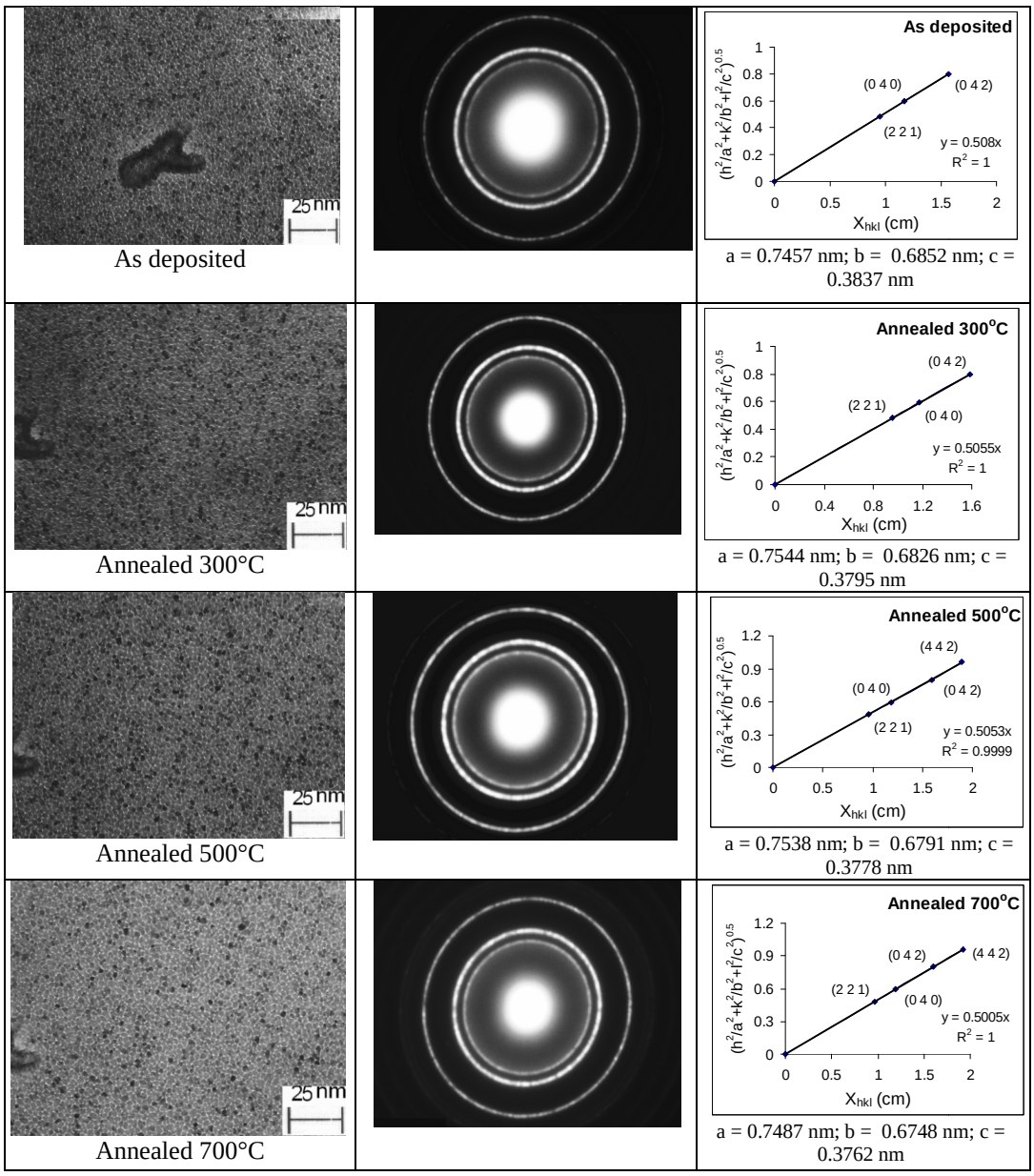

FIGURE 5
in situ TEM analysis of Ni_5Al_3 thin films showing the grain growth and corresponding SAD patterns.

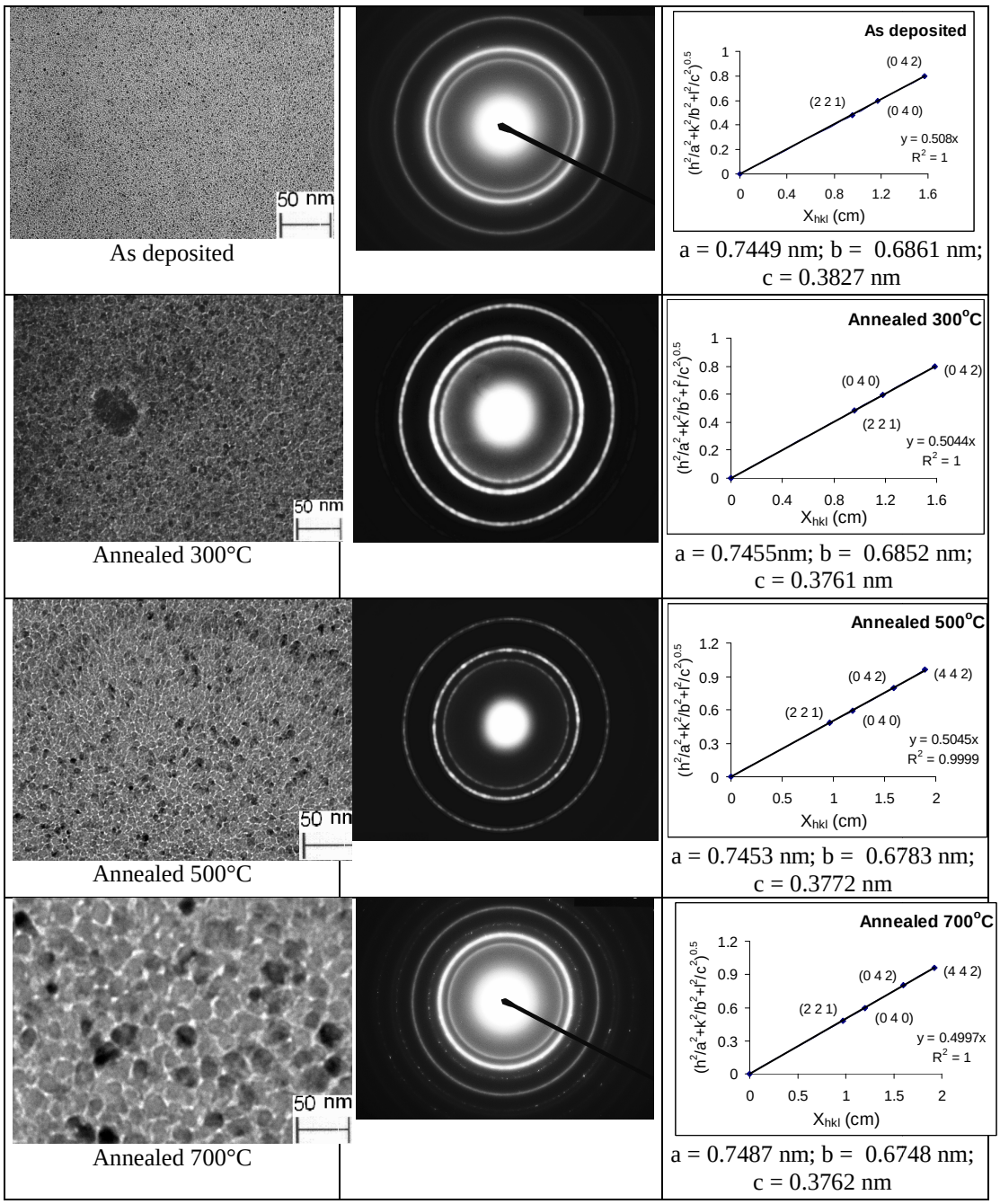

FIGURE 6
TEM analysis of post deposition annealed $Ni_{0.65}Al_{0.35}$ thin films and their SAD patterns.

4.0 DISCUSSION

A fairly interesting observation made in the present resistance study is the transition from positive to negative TCR in the Ni_5Al_3 films. The transition of TCR characters

observed in the current Ni_5Al_3 films at 170 °C is not a unique phenomenon but has been exhibited by some other systems including $La_{1-x}Sr_xMnO_3$ and $La_{1-x}Co_xMnO_3$ colossal magnetoresistance materials (PTC-NTC) (Grishin et al., 1999), (Khartsev et al. 2000) and polycrystalline $BaTiO_3$ and $(Sr_{1-x}Pb_x)TiO_3$ ferroelectric materials (NTC-PTC-NTC) as temperature increases (Lu and Tseng, 1998), (Zhao et al., 2001), (Shahrani and Abboudy, 2000). One of the potential explanations could be the effect of ferroelectricity or ferromagnetism - both phenomena have been identified to be the origin of the reported TCR transitions in the above mentioned oxide materials. As a matter of fact, ferromagnetic properties have been found to exist in nanocrystalline intermetallic aluminides (Qin et al., 1997), (Lin et al., 2005), (Varin et al., 1999), (Shi et al., 2008), which are otherwise paramagnetic in bulk forms. Therefore, it will be of scientific interest to further investigate the magnetic properties and their correlation to the TCR transition in the Ni_5Al_3 films.

By referring to the switching of PTC to NTC observed in our Ni_5Al_3 films, it is speculated that this can be related to a FM-PM transition as well. The magnetic properties of equilibrium Ni_5Al_3 are not well documented in the literature. So the type of magnetism and at where a FM-PM transition would occur, if applicable, remains unclear. However, when prepared in form of a nanocrystalline thin film, the magnetic properties of Ni_5Al_3 would not essentially the same as the bulk material. The emergence of such unexpected magnetic properties been attributed to the high surface-to-volume ratio of the nanograins, which leads to an increased chance of Ni-Ni ion coordinations where magnetic moments are originated. On the other hand, this intermetallic Ni_5Al_3 phase has an orthorhombic unit cell of Pt_5Ga_3-type with lattice parameters $a \approx b \approx 2c$ and is considered to consists of four differently ordered f.c.c unit cells. The observed lattice parameters show that ‘a’ and ‘b’ increase with increasing temperature as shown in Figure 1(c). A growth in the ‘a’ and ‘b’ directions would mean a large distortion and volume change.

From the present results we can conclude that Ni_5Al_3 alloy films are suitable for thin-film magnetoresistor based shape memory alloy applications. The present Ni-Al film offers a range of desirable properties as a magnetoresistor material. First of all, the positive TCR characteristics of the Ni_5Al_3 films, including the electrical resistance and conduction activation energy, are modifiable by annealing or control of film thickness. Accordingly, magnetoresistors with specific conductive sensitivities could be readily produced via suitable process control.

5.0 CONCLUSIONS

The thermal variations of magnetic cum electrical resistance of a range of Ni_5Al_3 sputter-deposited films were investigated. A positive TCR state was observed for Ni_5Al_3 alloy thin films. We have used two different dc-magnetron sputter systems

and the results were nearly the same. This proves that the positive TCR transition is characteristic of the Ni_5Al_3 alloy system in the thin-film state. These films are good candidate materials for applications as positive TCR magnetoresistor based shape memory alloys, with sensitivity tunable by annealing or thickness control.

6.0 REFERENCES

A. Gaur and G.D. Varma. 2008. Journal of Alloys and Compounds, 453 pp. 423-427.

A.M.Grishin, S.I. Khartsev, and P. Johnsson, 1999. Appl. Phys. Lett., 74 pp. 1015-1017.

A.A.Shahrani and S. Abboudy. 2000. J. Phys. Chem. Solids. 61 pp. 955-959.

A. Wolkenberg and T. Przesławski. 2006. Sensors and Actuators A 126 pp. 292–299.

B.V. Crist. 2000. Handbook of Monochromatic XPS Spectra: The Elements and Native Oxides, John Wiley & Sons.

D. Lin, J. Hu and D. Jiang. 2005. Intermetallics, 13 pp. 343-349.

H.P. Ng and A.H.W. Ngan. 2000. J. Appl. Phys., 88 pp. 2609 – 2616.

H. Shi, D. Guo and Y. Ouyang. 2008. J. of Alloys and Compounds, 455 pp. 207-209.

J.E. Castle. 2002. Surf. Interface Anal. 33. pp. 196-202.

J.H. Miao, S.L. Yuan, L. Yuan, G.M. Ren, X. Xiao, G.Q. Yu, Y.Q. Wang and S.Y. Yin. 2008. Mater. Res. Bull., 43 pp. 631-638.

J. Zhao, L. Li and Z. Gui. 2001. Sensors and Actuators A, 95 pp. 46-50.

Khartsev, S.I., Johnsson, P. and Grishin, A.M. 2000. J. Appl. Phys., 87 pp. 2394-2399.

M.Vopálenský, P. Ripka and A. Platil. 2003. Sensors and Actuators A 106 pp. 38–42.

P. Dimitrova, S. Andreev and L. Popova. 2008. Sensors and Actuators A 147 pp. 387–390.

P. Khadkikar and K. Vedula. 1987. compiled by JCPDS, file No. 40 – 1157. J. Mater. Res., 2. pp. 163.

R. A. Varin, J. Bystrzycki and A. Calka. 1999, Intermetallics, 7 pp. 917-930.

W. Huo and Y. Qu. 2006. Sensors and Actuators A, 128 pp. 265-269.

W.H. Han, X.K. Chen, E.Q. Xie, G. Wu, J.P. Yang, R. Wang, S.Z. Cao and Y.L. Wang. 2007. Surface Coating Technology, 201 pp. 5680-5683.

W.i Li, Z. Xu, R. Chu, P. Fu and J. Hao. 2009. J. of Alloys and Compounds. 482 pp. 137-140.

X.Y. Qin, J.R. Sun and L.D. Zhang. 1997. Nanostructured Materials, 9 pp. 623-626.

Y.L. Chan, K.W.K. Yeung, W.W. Lu, A.H.W. Ngan, K.D.K. Luk, D. Chan, S.L. Wu, X.M. Liu, Paul K. Chu and K.M.C. Cheung. 2007. Nucl. Instr. and Meth. in Phys. Res. B 257, pp. 687–691.

Y.L. Chan, S.L. Wu, X.M. Liu, Paul K. Chu, K.W.K. Yeung, W.W. Lu, A.H.W. Ngan, K.D.K. Luk, D. Chan and K.M.C. Cheung. 2007. Surf. Coat. Technol. 202, pp. 1308–1312.

Y.Y. Lu, and T.Y. Tseng, 1998. Mat. Chem. Phys., 53 pp. 132-137.